

The impact of the intrinsic charm quark content of the proton on differential $\gamma + c$ cross section

S. Rostami¹, A. Khorramian^{1,2}, A. Aleedaneshvar¹

¹ *Physics Department, Semnan University, Semnan, Iran,*

² *School of Particles and Accelerators, Institute for Research in Fundamental Sciences (IPM), P.O.Box 19395-5531, Tehran, Iran*

Abstract

We present a comparative analysis of the impact of the non-perturbative intrinsic charm quark content of the proton on differential cross section of $\gamma + c$ -jet in pp and $p\bar{p}$ collisions, for the kinematic regions that are sensitive to this contribution. We discuss the Q^2 evolution of intrinsic quark distributions at the next-to-leading order (NLO) and present a code which provide these distributions as a function of x and Q^2 for any arbitrary Fock state probability. For the $p\bar{p}$ collisions at the Tevatron, the results are compared with the recent experimental data of D0 at $\sqrt{s} = 1.96$ TeV and also predictions for pp collisions at $\sqrt{s} = 8$ TeV and $\sqrt{s} = 13$ TeV for the LHC.

1 Introduction

The parton distribution functions (PDFs) are essential to make precise prediction for the standard model (SM) processes at hadron colliders such as $p\bar{p}$ and pp scattering at Tevatron and LHC, respectively. Actually, the cross section of hadron-hadron scattering is explained in terms of parton-parton scattering which is the convolution of PDFs and partonic cross section. One of the important properties of these non-perturbative PDFs is that they are universal, i.e., they are the same in all kinds of processes. Precise knowledge of these PDFs describing the proton's quark and gluon content is very important to test the SM and to search for New Physics.

The parton distribution $f_i(x, Q^2)$ of the proton, is the number density of partons of flavour i carrying a momentum fraction x at energy scale Q^2 . Because the PDFs are non-perturbative objects, they cannot be determined directly from the first principles in QCD and have to be fixed by experimental information. The procedure is parametrizing the x dependence of PDFs at a scale Q_0^2 , where Q_0^2 has to be lie in the perturbative regime such that the known Dokshitzer-Gribov-Lipatov-Altarelli-Parisi (DGLAP) evolution equations are applicable [1–3].

According to DGLAP evolution equations, we are able to obtain the shape of the PDFs by fitting to the available data from experimental observables. In recent years, several theoretical groups have extracted PDFs by doing a QCD global analysis [4–15].

The QCD physics of heavy quarks in the proton is one of the most important purposes for the Electron-Ion Collider (EIC), and it has many important consequences for high energy colliders, including the Large Hadron Electron Collider (LHeC) at CERN. Recently a number of important processes, including heavy quarks production which are sensitive to charm and bottom quark distributions are presented [16–19]. Indeed, Fock states of the proton wave function with five quarks such as $uudq\bar{q}$ where $q = u, d, s$ and c, b has been considerably interested in recent years [20–34]. In this regards, many articles have studied non-perturbative “intrinsic” sea quark components in addition to the commonly perturbative “extrinsic” ones in the nucleon wave function, which the first time was suggested by Brodsky, Hoyer, Peterson, and Sakai (BHPS) in 1980 [35] (see Ref. [22] for a recent review).

There are remarkable differences between the extrinsic and intrinsic sea quarks. The extrinsic sea quarks arise in the proton perturbatively through the splitting of gluons into quark-antiquark pairs in the DGLAP Q^2 evolution and produce more and more when the Q^2 scale increases. Meanwhile extrinsic sea quarks dominate at very low parton momentum fraction x and so have a “sealike” characteristics. In contrast, the intrinsic sea quarks arise through the non-perturbative fluctuations of the nucleon state to five-quark states or virtual meson-baryon states in Meson Cloud Model (MCM) framework [29, 36] in the light-cone Fock space picture [37]. They exist over a time scale which is independent of any probe momentum transfer (infinite momentum frame). Moreover, the intrinsic sea quarks behave as “valencelike” quarks and then their distributions peak at relatively large x .

In addition to the BHPS, there have also been a number of theoretical calculations to describe the intrinsic charm (IC) distribution in the light cone framework. However, one can find a review of these models in Refs. [38, 39]. For example, the study of EMC charm leptonproduction data done by Harris, Smith and Vogt [40] indicated that an IC component with $0.86 \pm 0.6\%$ probability can be present in the nucleon. Also the CTEQ collaboration [41–43] studied the magnitude of the probability for intrinsic charm state within a global analysis of PDFs considering a wide range of the hard-scattering data. They showed that the probability for IC can be 2-3 times larger than the predicted value without any inconsistency with the experimental data. Recently, two global analyses about the importance of intrinsic charm have been performed. The first one, by the CTEQ collaboration [43], follows their previous work and the second one, by Jimenez-Delgado *et al.* [34] which using looser kinematic cuts for including low- Q and high- x data. Also in Refs. [44, 45] searches for intrinsic charm component of the proton at the LHC are presented. In this case, having a code which can

extract the intrinsic heavy densities for any arbitrary intrinsic quark probability would be valuable.

As mentioned before, some processes are sensitive to charm quark distributions in the large x region. For instance, the produced charm quark in deep inelastic lepton-proton scattering $lp \rightarrow l'cX$, which has been performed by the European Muon Collaboration (EMC) experiment [46]. As another example, the J/ψ hadroproduction at high x which was observed in pA and πA collision by NA3 at CERN [47] and E866 at FNAL [48]. Likewise, the inclusive production of charmed hadrons at hadron colliders at large x is a good laboratory to investigate the role of intrinsic charm in the proton. For example, the production of charmed hadrons in $pp \rightarrow DX$ and $pp \rightarrow \Lambda_c X$ observed at ISR [49] and at Fermilab [50, 51]. In addition to the above mentioned processes, the results of prompt photon production in association with a charm quark at hadron colliders ($pp(\bar{p}) \rightarrow \gamma + c\text{-jet}$) [17, 44] are dependent on the charm quark distribution. The contribution of the charm quark at large x can be studied also in the $c\text{-jet}$ production accompanied by vector bosons Z, W^\pm [18].

In the present study, we perform the Q^2 evolution of intrinsic quark distributions and present a code providing these distributions at any x and Q^2 values for any arbitrary Fock state probability. Besides we present a comparative analysis of IC contribution in the proton, using the production of $\gamma + c\text{-jet}$ in pp and $p\bar{p}$ collisions. Particular attention is paid to calculate the differential $\gamma + c\text{-jet}$ cross section. We can compare our results with the recent experimental data of D0 at $\sqrt{s} = 1.96$ TeV at the Tevatron. Also we present some predictions for pp collisions at $\sqrt{s} = 8$ TeV and $\sqrt{s} = 13$ TeV for the LHC. The outline of this paper is as follows. In section 2 we briefly review the light-cone model for intrinsic charm introduced by BHPS. The Q^2 -evolution of intrinsic quark distribution is presented in Sec. 3, where we compare the evolution of extrinsic and intrinsic charm distributions. In Sec. 4 we present our NLO predictions for production of $\gamma + c\text{-jet}$ in pp and $p\bar{p}$ collisions. Finally, in Sec. 5 we will summarize our results.

2 The light-cone picture of the proton and the BHPS model

The light cone formalism allows a proton to exist in various Fock configurations [52]. Therefore the wave function of the proton consists of $|uud\rangle$ distribution plus Fock states of n -particle given by number [53]

$$\begin{aligned} |p\rangle &= \psi_{3q/p}(\vec{k}_{\perp i}, x_i) |uud\rangle + \psi_{3qg/p}(\vec{k}_{\perp i}, x_i) |uudg\rangle \\ &+ \psi_{5q/p}(\vec{k}_{\perp i}, x_i) |uudq\bar{q}\rangle + \dots \end{aligned} \quad (1)$$

In the light cone framework for the wave function amplitudes of Fock components we have

$$\psi_{n/p}(\vec{k}_{\perp i}, x_i) \propto \frac{1}{M^2 - \sum_{i=1}^n \left(\frac{m_i^2 + k_{\perp i}^2}{x_i} \right)}, \quad (2)$$

where M is the mass of the proton and m_i and $k_{\perp i}$ are the mass and transverse momentum of parton i in the Fock state, respectively and x_i is the momentum fraction carrying by parton i that the momentum conservation is satisfied as follows

$$\sum_{i=1}^n \vec{k}_{\perp i} = \vec{0}_{\perp}, \quad \sum_{i=1}^n x_i = 1, \quad (3)$$

and the momentum distributions are determined from integrating the square of the wave function.

The possible existence of a five-quark Fock component $|uudq\bar{q}\rangle$ in the wave function of the proton for the first time presented by Brodsky, Hoyer, Peterson, and Sakai (BHPS) in 1980.

According to the BHPS model the probability distribution for the five-quark state assuming that the effect of transverse momentum is negligible, can be written as [35]

$$\begin{aligned} P(x_1, \dots, x_5) &= \mathcal{N} \delta(1 - \sum_{i=1}^5 x_i) [M^2 - \sum_{i=1}^5 \frac{m_i^2}{x_i}]^{-2} \\ &= \mathcal{N} \delta(1 - \sum_{i=1}^5 x_i) \left[M^2 - \frac{m_u^2}{x_1} - \frac{m_u^2}{x_2} - \frac{m_d^2}{x_3} - \frac{m_q^2}{x_4} - \frac{m_{\bar{q}}^2}{x_5} \right]^{-2}, \end{aligned} \quad (4)$$

where as mentioned above, m_i is the mass of the parton i in the Fock state and x_i is the momentum fraction carried by it. In the above equation, \mathcal{N} is the normalization factor and can be determined from

$$\mathcal{P}_5^{q\bar{q}} = \int_0^1 dx_1 \dots dx_5 P(x_1, \dots, x_5), \quad (5)$$

where $\mathcal{P}_5^{q\bar{q}}$ is the $|uudq\bar{q}\rangle$ Fock state probability. For the case that q is a heavy quark, namely c or b (which we denote here with Q), BHPS assumed the light quark and proton masses are negligible compared to the heavy quark mass. Therefore, in this limit the $|uudQ\bar{Q}\rangle$ Fock state probability distribution takes the form

$$P(x_1, \dots, x_5) = \mathcal{N}_5 \delta(1 - \sum_{i=1}^5 x_i) \frac{x_4^2 x_5^2}{(x_4 + x_5)^2}, \quad (6)$$

where $\mathcal{N}_5 = \mathcal{N}/m_{Q,\bar{Q}}^4$ and its value is determined from Eq. (5) so that $\mathcal{N}_5 = 3600 \mathcal{P}_5^{Q\bar{Q}}$. Finally, the probability distribution for the intrinsic heavy quark in the proton obtained by integrating over $dx_1 \dots dx_4$ is given by

$$P(x_5) = \mathcal{P}_5^{Q\bar{Q}} 1800 x_5^2 \left[\frac{(1-x_5)}{3} (1 + 10x_5 + x_5^2) + 2x_5(1+x_5) \ln(x_5) \right]. \quad (7)$$

According to Eq. (4) when we use the same value for the mass of q and \bar{q} , we obtain equal probability distributions for them in the five-quark state of the proton. According to BHPS [35] assumption with 1% probability for intrinsic charm (IC) in the proton we have

$$c(x) = 18x^2 \left[\frac{(1-x)}{3} (1 + 10x + x^2) + 2x(1+x) \ln(x) \right], \quad (8)$$

where for convenience, we used x in place of x_5 . Although an estimation of the order of 1% for the probability of finding intrinsic charm in the proton have been found before [35, 54], but the first detailed global analysis of PDFs including the intrinsic charm component were performed by CTEQ [42]. In Ref. [42] the probability for IC can be 2-3 times larger than previous predictions. Most recently, two global analyses estimated the probability of IC and they reached different conclusions about the possibility of IC. The first one presented by CTEQ collaboration [43] using CT10 framework [2]. According to this reference, a broader possible probability value for IC is 2.5%. The second one, presented by Jimenez-Delgado *et al.* [34], they found that the value of IC is at most 0.5%. There are some differences between these two QCD analyses. In Ref. [34], they used less restrictive kinematical cuts $Q^2 \gtrsim 1 \text{ GeV}^2$ and $W^2 \gtrsim 3.5 \text{ GeV}^2$ in their analysis in contrast to the previous works. These changes in kinematical cuts lead to a large number of SLAC data related to the lower Q^2 and W^2 , that might be sensitive to the IC contribution, to be included in QCD fit. In addition, in Ref. [34], they have included EMC heavy structure function F_2^c data [46] which can be a possible evidence for existence of the intrinsic charm quark. Using various data in these two

global analyses of PDFs, affected the obtained results of IC probability from these analyses. As we will demonstrate in this paper, D0 data can be another evidence for IC contribution. So including these data in a global QCD fit could help place additional bounds on IC probability. Although the determination of IC contribution must be done in a global QCD fit but, with using the discussed technique in this paper, for investigating the impact of IC on physical observables, we can change the amount of IC contributions without performing a complete global analysis for each case. In the present study, in addition to 1% IC, we choose the value of 3.5% IC to investigate the impact of upper limit of IC on the physical observables such as photon production in association with a charm quark. However, it should be noted that the actual value of IC which is more likely lower than 3.5, would be more reasonable.

According to Eq. (7), the distribution of the intrinsic bottom (IB) quarks and intrinsic charm quarks are identical. But it is different in the value of normalization. The probability for IB is expected to be $\mathcal{P}_5^{bb} = \mathcal{P}_5^{c\bar{c}}(m_c^2/m_b^2) \sim 0.001$ (with $\mathcal{P}_5^{c\bar{c}} = 0.01$) where $m_c \simeq 1.3$ GeV and $m_b \simeq 4.2$ GeV are the masses of charm and bottom quarks, respectively. As the probability of finding IB in the proton is smaller than IC by a factor of 0.1, the experimental search for finding an IC signature in $pp(\bar{p})$ collisions is more interested than IB.

To calculate the intrinsic light quark distributions we can not neglect the mass of the proton and light quarks. In this regard, we need to compute the Eq. (4) numerically. Recently, Chang and Peng [55] calculated the intrinsic quarks distribution using Monte Carlo techniques and then extracted the probabilities for the intrinsic light quark Fock states. In this work, we also calculate the intrinsic quark distributions without any assumptions to neglect the proton and light quarks masses. To check our method, for the case of intrinsic charm we used $m_p = m_u = m_d = 0$ in our calculation and we found the result completely equal to Eq. (8). In this way, for the case of intrinsic strange quark, we choose $m_u = m_d = 0.3$ GeV for the mass of u and d quarks and $m_s = 0.5$ GeV for the mass of s quark. The parametrization form is given by

$$s(x) = \mathcal{P}_5^{s\bar{s}} \times 13188.9 x^{1.627} (1-x)^{10.152} (0.029 + x^{3.713} + x^{7.426}). \quad (9)$$

3 The evolution of intrinsic quark distributions

Heavy quarks play a crucial role in the study of many processes such as single-top production and Higgs production in the standard model and beyond which are quite sensitive to the heavy quark content [41]. Furthermore, having a precise knowledge about the heavy quark components can help to understand the fundamental structure of the nucleon. In the standard global analysis of PDFs, heavy quarks distribution are assumed zero for $Q^2 < m_Q^2$. In this way, we do not need any parameterization form for the heavy quark distributions and they arise perturbatively through the splitting of gluons into quark-antiquark pairs in DGLAP Q^2 -evolution equations. Moreover, in these analysis it is usually assumed that there is no intrinsic heavy quark IQ in the proton. Although there is no theoretical reason to reject this assumption, there are some data that suggest the existence of an intrinsic heavy component in the proton [46]. In addition to the experimental evidence, in the light-cone picture of the proton the existence of the intrinsic components in the proton wave function is inevitable; these kinds of quarks are certainly non-perturbative in origin and can play an important role at high x . Therefore, in order to investigate the impact of intrinsic heavy quarks on the physical observables, the study of the evolution of their distributions together with extrinsic ones can be interesting and useful study.

Since the intrinsic heavy quark distribution gives an insignificant contribution to the evolution of light quark and gluon distributions, one can use the standard approach for global analysis of PDFs without considering an intrinsic heavy quark component in gluon and light quark distributions.

The DGLAP evolution equation that used for the standard approach of global analysis has compact form as [1–3]

$$\dot{f}_i = \sum_{j=q,g,Q} P_{ij} \otimes f_j. \quad (10)$$

For the heavy quark distribution, the scenario is different. If we adopt the intrinsic quarks in the proton, then the total heavy quark distribution in any x and Q^2 region can be obtained by adding the intrinsic contribution (non-perturbative) xQ_{int} to the extrinsic component (perturbative) xQ_{ext} as follows

$$xQ(x, Q^2) = xQ_{ext}(x, Q^2) + xQ_{int}(x, Q^2), \quad (11)$$

where $Q = c, b$ and we use the short-hand notation $xQ(x, Q^2) \equiv xf_Q(x, Q^2)$. It should be noted that it is not possible to mix these two terms in the boundary conditions for the QCD evolution. In this case, the evolution equation of heavy quarks can be separated into two independent parts. The first part is evolution of the extrinsic heavy quark. The PDFs for the extrinsic heavy component, like gluon and light quark, can be taken from a global analysis result of various groups providing global analysis of PDFs [5–8, 10–12], for example CTEQ66 [42] which are available in the Les Houches Accord PDF Interface (LHAPDF [56]) in arbitrary x and Q^2 . The second part is evolution of the intrinsic heavy quark distribution Q_{int} . The Q^2 -evolution of the intrinsic heavy quark distribution is controlled by non-singlet evolution equation. According to Ref. [20], non-singlet evolution provides a good approximation for evolution of the intrinsic heavy quark distributions as

$$\dot{Q}_{int} = P_{QQ} \otimes Q_{int}. \quad (12)$$

Therefore, non-singlet technique allows us to evolve intrinsic heavy quark distribution independently from the gluon and other PDFs. We should care the momentum sum rule for all PDFs in a global QCD analysis, if we take into account the above non-singlet evolution equation for intrinsic heavy quarks. But as discussed in Ref. [20], we have very small violation of this sum rule for intrinsic heavy quarks.

In recent years the CTEQ collaboration has done some global analysis of PDFs considering intrinsic charm from the BHPS model [35] by adding its contribution for $Q \geq m_c$ to the charm content of the proton and presented CTEQ66c PDF sets [42] for intrinsic quark. By using their results, we can only have the total charm distribution in any x and Q^2 but we do not have the intrinsic contribution separately. whereas non-singlet evolution of the intrinsic heavy quark component of the parton allows us to study the impact of this nonperturbative contribution on the physical observable without performing a complete global analysis of PDFs. In other word, this technique gives us evolution of the intrinsic charm distribution in any x and Q^2 and can be added to any PDFs. We carried out our calculation by QCDNUM package [57] and used its ability for the evolution of the non-singlet PDFs.

Fig. 1 shows the x distribution of extrinsic charm from the CTEQ66 [42] and intrinsic charm with 1% and 3.5% probability by the method we described above at $Q^2 = 1.69, 100$ and 10000 GeV^2 . In this figure, we also present the total charm distribution which is the sum of extrinsic and intrinsic components (1% and 3.5%). As can be seen, the intrinsic distribution starts from zero and its behaviour is like the valence distributions so that if we integrate it, we can obtain $\mathcal{P}_5^{c\bar{c}}$. To check the evolution, one can extract the extrinsic charm distribution at fixed Q^2 using CTEQ66 PDFs and then add it to IC contribution using our grids to compare this total charm distribution with extracted results from CTEQ66c [42]. This comparison shows that, there is a good agreement between our result and CTEQ66c. As a result of the evolution of intrinsic distribution, one can see that the intrinsic distribution's peak decreases in magnitude and also shifts to the smaller values of x just like the valence quark behaviour as expected. The Q^2 -evolution of the extrinsic charm distribution is dominated at small x

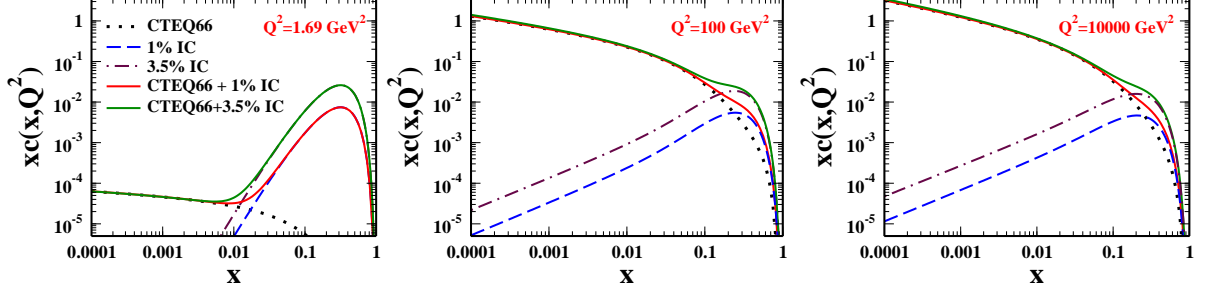


Figure 1: Distributions of the charm quark in the proton. The dotted curve shows the extrinsic charm distribution from CTEQ66 at $Q^2 = 1.69, 100$ and 10000 GeV^2 [42]. The dashed blue and dotted-dashed maroon curves correspond to our results for the 1% and 3.5% intrinsic charm distribution at mentioned Q^2 values. The solid red curve displays the total charm distribution considering a 1% IC from our grid plus CTEQ66 PDFs and the solid green curve presents the total charm distribution considering a 3.5% IC from our grid plus CTEQ66 PDFs.

and have a sea like behaviour so that at higher Q^2 , its magnitude increases at small x in the DGLAP evolution regime. Thus, the Q^2 -evolution of the total charm distribution in the proton containing extrinsic contribution from CTEQ66 [42] and intrinsic ones from the BHPS [35] increases at small x and decreases at high x at higher Q^2 . Our results are compatible with very recently reported results in Ref. [20]. It should be noted that we use NLO extrinsic PDFs from CTEQ66 sets [42] and our calculations for IC non-singlet evolution are performed at the NLO approximation as well.

Actually, the significant difference between our work and CTEQ66c is that, in our work there is no limitation to choose the value of $\mathcal{P}_5^{c\bar{c}}$. Thus, one can have the x distribution of intrinsic charm for any $\mathcal{P}_5^{c\bar{c}}$ at arbitrary Q^2 .

Since having the evolution of intrinsic quark distributions are important at large momentum fraction x , we prepare a set of grid files for the intrinsic strange, charm and bottom distributions and also an interpolation code to evolve these distributions to any x and Q^2 values [58]. It should be noted that, one can choose and fix the value for the probability of intrinsic quark $\mathcal{P}_5^{q\bar{q}}$ as an input parameter.

4 The prompt photon production in association with a c-jet

The prompt photon production in association with charm quark jet process can provide some information of parton distribution functions and improve our understanding of the perturbative techniques applied to calculate the hard scattering sub-process and also investigate the possibility of intrinsic charm quark component in the proton at larger x [44]. According to Fig. 2, at the leading order (LO), the main contribution arises from the Compton sub-process $gc \rightarrow \gamma c$. Within the leading order, the inclusive $\gamma + c$ production can also originate from the sub-processes $gg \rightarrow c\bar{c}\gamma$, $cg \rightarrow cg\gamma$ or $qc \rightarrow qc\gamma$ where the fragmentation of quarks or gluons produces a photon.

At the next-to-leading order (NLO), the number of contributing sub-processes increases. In this way, the photon component includes contributions from $gg \rightarrow \gamma c\bar{c}$, $gc \rightarrow \gamma gc$, $cq \rightarrow \gamma qc$, $c\bar{q} \rightarrow \gamma \bar{q}c$, $c\bar{c} \rightarrow \gamma c\bar{c}$, $cc \rightarrow \gamma cc$ and the annihilation sub-process $q\bar{q} \rightarrow \gamma c\bar{c}$ [59, 60], which apart from $q\bar{q} \rightarrow \gamma c\bar{c}$, all sub-processes are g and c PDF initiated. At the LHC, the Compton process dominates for all energies, whereas at the Tevatron the annihilation process $q\bar{q} \rightarrow \gamma c\bar{c}$ dominates for photons with high transverse momentum p_T^γ [59].

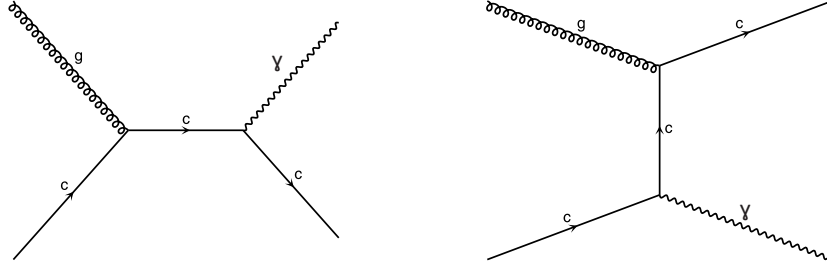


Figure 2: The Feynman diagrams for the QCD leading order contribution of the Compton process $gc \rightarrow \gamma c$ in the s-channel (left) and in the t-channel (right).

4.1 Comparison to Tevatron data

Recent years, the prompt photon and heavy quark jet production in $p\bar{p}$ collisions at the Tevatron have been investigated [16, 17, 61, 62]; this process can be very useful for testing the possible existence of intrinsic quarks in the nucleon. For example, in Ref. [17] the differential cross section for the associated production of a c -quark jet and an isolated photon with rapidity $|y^\gamma| < 1.0$ and transverse momentum $30 < p_T^\gamma < 300$ GeV have been measured as a function of p_T^γ at $\sqrt{s} = 1.96$ TeV so that the c -jet has $|\eta^c| < 1.5$ and $p_T^c > 15$ GeV.

Fig. 3 shows a comparison of the D0 measurement of the differential $\gamma + c$ -jet cross section as a function of p_T^γ [17] and the corresponding NLO theoretical calculation. This calculations have been carried out by the MadGraph [63]. The lowest curve is related to CTEQ66 PDFs [42] without the IC contribution and as it is clear, it has a poor description of data. At large p_T^γ region, as expected, the spectrum grows by the inclusion of the IC contribution. In this figure the solid, dashed and dotted-dashed curves represent the theoretical results for the cross section using the CTEQ66 [42] (without IC contribution) and CTEQ66 plus BHPS with 1% and 3.5% IC, respectively. One can see the obtained result considering 3.5% IC has the better description of data. In the bottom of Fig. 3, the ratio of CTEQ66 PDFs adding 1% and 3.5% IC to CTEQ66 PDFs is illustrated. This ratio for 3.5% IC is about 1.5 when p_T^γ reaches 216 GeV, while this factor for a 1% IC contribution is about 1.2. Also, in the bottom of Fig. 3, we showed the ration of data to the result of CTEQ66 plus 3.5% IC by yellow points.

Although, we could also use the CTEQ66c PDFs but as mentioned in previous section, we can choose any value for $\mathcal{P}_5^{c\bar{c}}$ in our calculation. Using CTEQ66c PDFs and our results in this calculation are in good agreement with each other.

4.2 Predictions for the LHC

The LHC with pp -collisions, operate at the center of mass energy, $\sqrt{s} = 7 - 14$ TeV, which is much greater than the Tevatron. In order to make prediction of the inclusive production of $\gamma + c$ -jet process at the LHC, we need to select kinematical regions where are the most sensitive to the intrinsic charm quark contribution. To this, we have used the kinematical regions which analyzed in detail by V. A. Bednyakov *et al.* [44].

The differential $\gamma + c$ -jet cross section in pp collisions versus the transverse momentum of the photon is presented for the photon rapidity $1.52 < |y^\gamma| < 2.37$ at $\sqrt{s} = 8$ TeV and for transverse momentum $50 < p_T^\gamma < 400$ GeV. The c -jet also has $|\eta^c| < 2.4$ and $p_T^c > 20$ GeV. In this kinematical region, the charm momentum fraction is larger than 0.1 ($x_c > 0.1$) where the intrinsic charm distribution is completely considerable in comparison with the extrinsic charm distribution.

In Fig. 4 the differential cross section $d\sigma/dp_T^\gamma$ for $pp \rightarrow \gamma + c$ -jet process calculated at NLO is presented as a function of the transverse momentum of photon. In this kinematic region, considering IC contribution can substantially increase the cross section values especially at high p_T^γ . In this figure we present the results using CTEQ66 and CTEQ66 plus 1% IC.

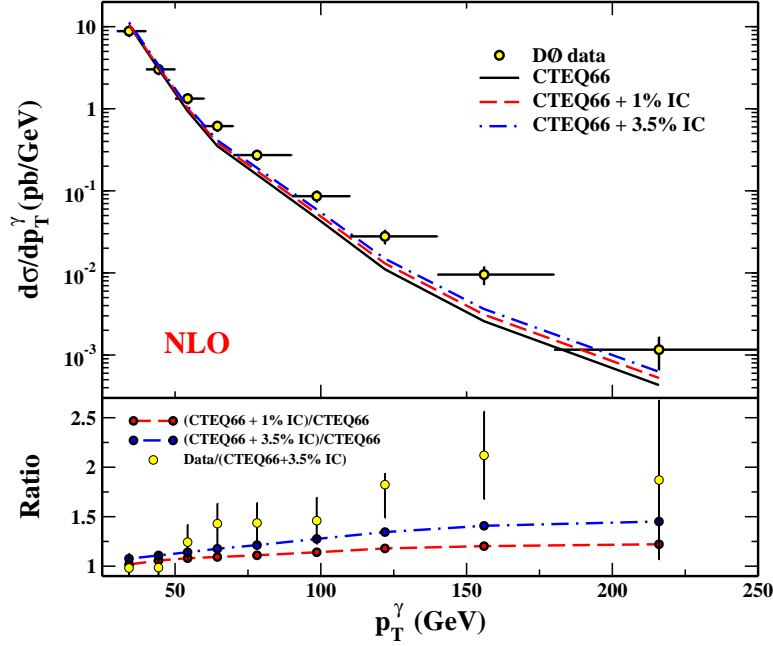


Figure 3: A comparison of D0 measurement of differential $\gamma + c$ -jet cross section as a function of p_T^γ at $\sqrt{s} = 1.96$ TeV with $|\eta^c| < 1.5$ and $|y^\gamma| < 1.0$ [17] and corresponding the NLO theoretical calculations. The solid curves are calculated using CTEQ66 (pure extrinsic) [42]. The dashed and dotted-dashed curves correspond to the inclusion of 1% and 3.5% IC from the BHPS, respectively and using our grids files [58](top). The ratio of these spectra (including IC contribution) to the pure extrinsic CTEQ66 is shown in the bottom panel. The ratio of $\gamma + c$ -jet cross sections for data to CTEQ66 plus 3.5% IC presented by yellow points.

Moreover for the comparison, we present the results obtained using CTEQ66 plus 3.5% IC. The difference between the results is clearly visible in bottom of Fig. 4 where the ratio of the spectra including IC contribution with 1% and 3.5% IC probability to CTEQ66 is presented as a function of p_T^γ . By comparing the results, one can recognize that the values of the spectra increases considering IC contribution so that the BHPS with 3.5% IC result is placed above the CTEQ66 and CTEQ66 plus 1% IC. For example, the inclusion of the 3.5% IC increases the spectrum by a factor of 2.8 at $p_T^\gamma = 380$, while for the 1% IC this factor is about 1.6. Our results for the differential cross section of $pp \rightarrow \gamma + c$ -jet process at $\sqrt{s} = 8$ TeV are in good agreement with recent published results [44].

To further investigate the role of intrinsic charm in the proton, we give predictions for the LHC, but at the center of mass energy $\sqrt{s} = 13$ TeV. Therefore, we used the kinematical regions which is presented in Ref. [44]. According to Ref. [44] we have

$$x_c \geq x_F = \frac{2p_T}{\sqrt{s}} \sinh(\eta), \quad (13)$$

where x_F is the Feynman scaling variable of the produced hadron and x_c is scaling variable of the intrinsic charm quark in the proton. As well as, η is pseudo rapidity of photon and p_T is its transverse momentum. According to presented kinematic cut at $\sqrt{s} = 8$ TeV by V. A. Bednyakov et al. [44] for $x_c \geq 0.1$, the values of the photon transverse momentum p_T will be changed by a factor 13/8 for the photon rapidity $1.52 < |y^\gamma| < 2.37$ and transverse momentum $50 < p_T^\gamma < 400$ GeV at $\sqrt{s} = 13$ TeV.

The differential cross section $d\sigma/dp_T^\gamma$ for $pp \rightarrow \gamma + c$ -jet process calculated at NLO as a function of transverse momentum of the photon has been shown in the Fig.5. Here, we choose the rapidity of photon and c -jet, $1.52 < |y^\gamma| < 2.37$ and $|\eta^c| < 2.4$, respectively. We use also the $p_T^c > 20$ GeV and $80 < p_T^\gamma < 540$ GeV for c -jet and photon transverse momentum.

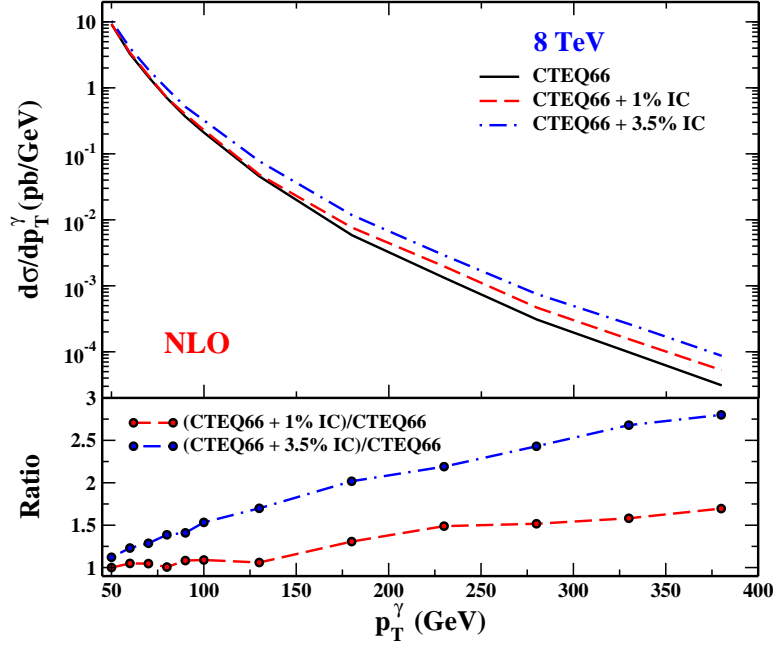


Figure 4: The differential $\gamma + c$ -jet cross section in pp collisions as a function of p_T^γ for NLO theoretical calculations at $\sqrt{s} = 8$ TeV and using CTEQ66 without IC contribution (solid curve), CTEQ66 [42] plus 1% (dashed curve) and 3.5% (dotted-dashed curve) IC from grid files [58] (top). The ratio of these spectra (including IC contribution) to the pure extrinsic CTEQ66 is shown in the bottom panel.

Similar way to our result for $\sqrt{s} = 8$ TeV, the IC contribution can substantially increase the cross section values specially at high p_T^γ at $\sqrt{s} = 13$ TeV. The solid and dashed curves represent the calculation results using CTEQ66 and CTEQ66 plus 1% IC, respectively. Moreover, the result obtained using CTEQ66 plus 3.5% IC from the BHPS presented by dotted-dashed line. The difference between the results is clearly visible in bottom of Fig. 5 where the ratio of the spectra including IC contribution with 1 and 3.5% IC probability and without it, is presented as a function of p_T^γ . One can see the values of the spectra increase considering IC contribution. In this way, the inclusion of the 3.5% IC increases the spectrum by a factor 2.17 at $p_T^\gamma = 380$ GeV, while for the 1% IC this factor is about 1.34. Also this factor at $p_T^\gamma = 540$ GeV for 1 and 3.5% IC is about 1.46 and 2.45, respectively.

According to Eq. 13, at the specific values of the pseudo rapidity and the transverse momentum of the photon, by increasing the IC, \sqrt{s} decreases. For example, at $p_T^\gamma = 280$ GeV the spectrum increases by a factor 1.51 for $\sqrt{s} = 8$ TeV and 1.21 for $\sqrt{s} = 13$ TeV at the LHC. In addition, we should be noted that at the higher rapidity with a lower center-of-mass energy, where x_c would be larger and so the IC contribution in the proton is increased would be preferably suited to searching and discover intrinsic charm. Finally, we should mentioned that the cross section result using CT10 PDFs are very similar to the result of CTEQ66, but these values for MSTW are slightly higher than CTEQ66.

5 Conclusions

In this work, we present the evolution of intrinsic charm distribution which is practical for intrinsic bottom and strange quark. An important aspect of our calculation is that we present $x_{c_{int}}$ as a function of Q^2 for arbitrary $\mathcal{P}_5^{c\bar{c}}$. The grid files for the evolution of intrinsic strange, charm and bottom quarks for arbitrary $\mathcal{P}_5^{q\bar{q}}$ that were used in this paper are available in Ref. [58]. We have presented a comparative analysis to investigate the role of intrinsic charm

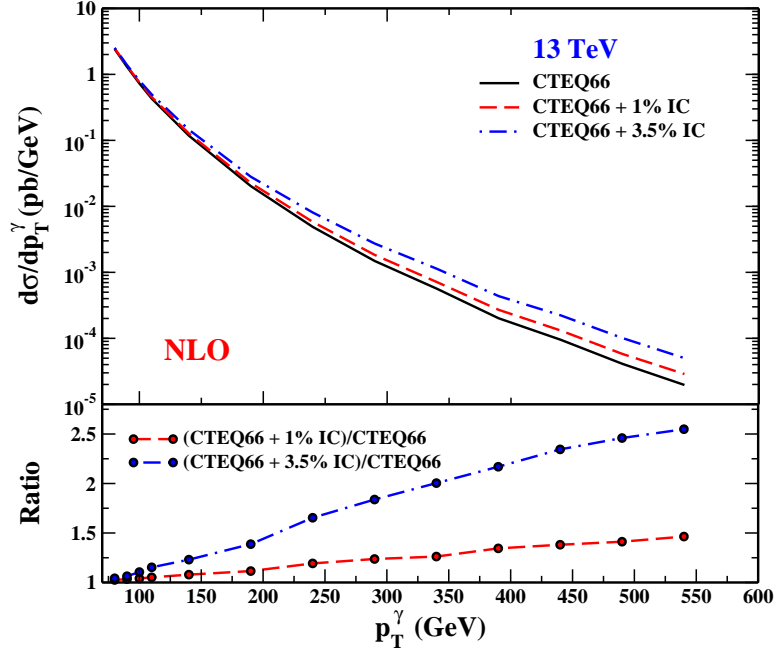


Figure 5: The differential $\gamma + c$ -jet cross section in pp collisions as a function of p_T^γ at the NLO and $\sqrt{s} = 13$ TeV and using CTEQ66 without IC contribution (solid curve), CTEQ66 plus 1% IC (dashed curve), CTEQ66 plus 3.5% IC (dotted-dashed curve), for forward photon rapidity $1.52 < |y^\gamma| < 2.37$ (top). The ratio of these spectra for 1% (dashed curve) and 3.5% (solid curve) IC contribution to CTEQ66 is shown in the bottom panel.

in the results of the inclusive production of a prompt photon and c -jet in hadron colliders for two value of $\mathcal{P}_5^{c\bar{c}}$. The calculations were done for the Tevatron $p\bar{p}$ -collisions at rapidity $|y^\gamma| < 1$, $|\eta^c| < 1.5$ and LHC pp -collisions at rapidity $1.52 < |y^\gamma| < 2.37$ and $|\eta^c| < 2.4$ at $\sqrt{s} = 8$ TeV and $\sqrt{s} = 13$ TeV. As a result we found, regardless of the value of intrinsic charm probability in the proton, the IC contribution increases the magnitude of the cross section, and has significant contribution in cross section when the photon transverse momentum grows. Finally, we have found that the BHPS with 3.5% IC has better compatible to the D0 data than 1% IC. Nevertheless, to determine the probability of the intrinsic charm component in the proton, a global analysis using D0 and LHC data (which are particularly sensitive to the charm quark) is required. We expect that using these data will give a better understanding of the IC components in the proton.

6 Acknowledgments

We thank S. J. Brodsky and F. Olness for reading manuscript and useful discussions and comments. S. R. appreciates O. Mattelaer, G. Lykasov and V. Bednyakov for discussion and help. A. K. thanks SITP (Stanford Institute for Theoretical Physics) and the Physics Department of SMU (Southern Methodist University) for their hospitality at the beginning of this work. He is also grateful to CERN TH-PH division for the hospitality where a portion of this work was performed.

A Fortran code

A FORTRAN package containing the distribution of intrinsic charm (IC) and bottom (IB) distributions and also intrinsic strange (IS) distribution for arbitrary x and Q^2 can be found

in <http://particles.ipm.ir/links/QCD.htm> [58] or obtained via e-mail from the authors. It should be noted that, this code is available for arbitrary $\mathcal{P}_5^{q\bar{q}}$. The package includes an example program to illustrate the use of the routines.

References

- [1] G. Altarelli and G. Parisi, Nucl. Phys. B **126**, 298 (1977).
- [2] V. N. Gribov and L. N. Lipatov, Sov. J. Nucl. Phys. **15**, 438 (1972) [Yad. Fiz. **15**, 781 (1972)].
- [3] Y. L. Dokshitzer, Sov. Phys. JETP **46**, 641 (1977) [Zh. Eksp. Teor. Fiz. **73**, 1216 (1977)].
- [4] L. A. Harland-Lang, A. D. Martin, P. Motylinski and R. S. Thorne, arXiv:1412.3989 [hep-ph].
- [5] J. Gao, M. Guzzi, J. Huston, H. L. Lai, Z. Li, P. Nadolsky, J. Pumplin and D. Stump *et al.*, Phys. Rev. D **89**, no. 3, 033009 (2014) [arXiv:1302.6246 [hep-ph]].
- [6] A. D. Martin, W. J. Stirling, R. S. Thorne and G. Watt, Eur. Phys. J. C **63**, 189 (2009) [arXiv:0901.0002 [hep-ph]].
- [7] L. Del Debbio *et al.* [NNPDF Collaboration], JHEP **0703**, 039 (2007) [hep-ph/0701127].
- [8] R. D. Ball, V. Bertone, S. Carrazza, C. S. Deans, L. Del Debbio, S. Forte, A. Guffanti and N. P. Hartland *et al.*, Nucl. Phys. B **867**, 244 (2013) [arXiv:1207.1303 [hep-ph]].
- [9] C. Bourrely and J. Soffer, arXiv:1502.02517 [hep-ph].
- [10] S. Alekhin, J. Bluemlein and S. Moch, Phys. Rev. D **89**, no. 5, 054028 (2014) [arXiv:1310.3059 [hep-ph]].
- [11] P. Jimenez-Delgado and E. Reya, Phys. Rev. D **89**, no. 7, 074049 (2014) [arXiv:1403.1852 [hep-ph]].
- [12] H. Khanpour, A. N. Khorramian and S. A. Tehrani, J. Phys. G **40**, 045002 (2013) [arXiv:1205.5194 [hep-ph]].
- [13] A. Kusina, K. Kovaik, T. Jeo, D. B. Clark, F. I. Olness, I. Schienbein and J. Y. Yu, PoS DIS **2014**, 047 (2014) [arXiv:1408.1114 [hep-ph]].
- [14] F. Arbabifar, A. N. Khorramian and M. Soleymaninia, Phys. Rev. D **89**, no. 3, 034006 (2014) [arXiv:1311.1830 [hep-ph]].
- [15] A. N. Khorramian, S. Atashbar Tehrani, S. Taheri Monfared, F. Arbabifar and F. I. Olness, Phys. Rev. D **83**, 054017 (2011) [arXiv:1011.4873 [hep-ph]].
- [16] V. M. Abazov *et al.* [D0 Collaboration], Phys. Lett. B **714**, 32 (2012) [arXiv:1203.5865 [hep-ex]].
- [17] V. M. Abazov *et al.* [D0 Collaboration], Phys. Lett. B **719**, 354 (2013) [arXiv:1210.5033 [hep-ex]].
- [18] V. M. Abazov *et al.* [D0 Collaboration], Phys. Rev. Lett. **112**, no. 4, 042001 (2014) [arXiv:1308.4384 [hep-ex]].
- [19] V. M. Abazov *et al.* [D0 Collaboration], Phys. Lett. B **737**, 357 (2014) [arXiv:1405.3964 [hep-ex]].

- [20] F. Lyonnet, A. Kusina, T. Jeo, K. Kovark, F. Olness, I. Schienbein and J. Y. Yu, JHEP **1507**, 141 (2015) [arXiv:1504.05156 [hep-ph]].
- [21] F. Lyonnet, A. Kusina, K. Kovak, T. Jeo, F. Olness, I. Schienbein and J. Y. Yu, arXiv:1507.08935 [hep-ph].
- [22] S. J. Brodsky, A. Kusina, F. Lyonnet, I. Schienbein, H. Spiesberger and R. Vogt, Adv. High Energy Phys. **2015**, 231547 (2015) [arXiv:1504.06287 [hep-ph]].
- [23] S. J. Brodsky and S. Gardner, arXiv:1504.00969 [hep-ph].
- [24] J. P. Lansberg and H. S. Shao, Nucl. Phys. B **900**, 273 (2015) [arXiv:1504.06531 [hep-ph]].
- [25] R. D. Ball, V. Bertone, M. Bonvini, S. Forte, P. G. Merrild, J. Rojo and L. Rottoli, arXiv:1510.00009 [hep-ph].
- [26] A. Vafaei, A. Khorramian, S. Rostami, A. Aleedaneshvar and M. Goharipour, Contribution to the Proceedings of QCD 15, Montpellier, July 2015.
- [27] S. Rostami, A. Khorramian, A. Aleedaneshvar and M. Goharipour, PoS EPS-HEP2015 (2015) 511.
- [28] J. Speth and A. W. Thomas, Adv. Nucl. Phys. **24**, 83 (1998).
- [29] S. Kumano, Phys. Rep. **303**, 183 (1998).
- [30] R. Vogt, Prog. Part. Nucl. Phys. **45**, S105 (2000).
- [31] G. T. Garvey and J.-C. Peng, Prog. Part. Nuc. Phys. **47**, 203 (2001).
- [32] W.-C. Chang and J.-C. Peng, Phys. Rev. Lett. **106**, 252002 (2011).
- [33] J.-C. Peng and J.-W. Qiu, Prog. Part. Nucl. Phys. **76**, 43 (2014).
- [34] P. Jimenez-Delgado, T. J. Hobbs, J. T. Londergan and W. Melnitchouk, arXiv:1408.1708 [hep-ph].
- [35] S. J. Brodsky, P. Hoyer, C. Peterson, N. Sakai, Phys. Lett. B **93**, 451 (1980); S.J. Brodsky, C. Peterson, N. Sakai, Phys. Rev. D **23**, 2745 (1981).
- [36] A. W. Thomas, Phys. Lett. B **126**, 97 (1983).
- [37] S. J. Brodsky, hep-ph/0412101.
- [38] J. Pumplin, Phys. Rev. D **73**, 114015 (2006) [hep-ph/0508184].
- [39] T. J. Hobbs, J. T. Londergan and W. Melnitchouk, Phys. Rev. D **89**, no. 7, 074008 (2014) [arXiv:1311.1578 [hep-ph]].
- [40] B. W. Harris, J. Smith and R. Vogt, Nucl. Phys. B **461**, 181 (1996) [hep-ph/9508403].
- [41] J. Pumplin, H. L. Lai and W. K. Tung, Phys. Rev. D **75**, 054029 (2007) [hep-ph/0701220].
- [42] P. M. Nadolsky, H. L. Lai, Q. H. Cao, J. Huston, J. Pumplin, D. Stump, W. K. Tung and C.-P. Yuan, Phys. Rev. D **78**, 013004 (2008) [arXiv:0802.0007 [hep-ph]].
- [43] S. Dulat, T. J. Hou, J. Gao, J. Huston, J. Pumplin, C. Schmidt, D. Stump and C.-P. Yuan, Phys. Rev. D **89**, no. 7, 073004 (2014) [arXiv:1309.0025 [hep-ph]].

- [44] V. A. Bednyakov, M. A. Demichev, G. I. Lykasov, T. Stavreva and M. Stockton, Phys. Lett. B **728**, 602 (2014).
- [45] P. H. Beauchemin, V. A. Bednyakov, G. I. Lykasov and Y. Y. Stepanenko, arXiv:1410.2616 [hep-ph].
- [46] J. J. Aubert *et al.* [European Muon Collaboration], Nucl. Phys. B **213**, 31 (1983).
- [47] J. Badier *et al.* [NA3 Collaboration], Z. Phys. C **20**, 101 (1983).
- [48] M. J. Leitch *et al.* [NuSea Collaboration], Phys. Rev. Lett. **84**, 3256 (2000) [nucl-ex/9909007].
- [49] P. Chauvat *et al.* [R608 Collaboration], Phys. Lett. B **199**, 304 (1987).
- [50] E. M. Aitala *et al.* [E791 Collaboration], Phys. Lett. B **495**, 42 (2000) [hep-ex/0008029].
- [51] E. M. Aitala *et al.* [Fermilab E791 Collaboration], Phys. Lett. B **539**, 218 (2002) [hep-ex/0205099].
- [52] G. P. Lepage and S.J. Brodsky, Phys. Lett. B **87**, 359 (1979); Phys. Phys. Rev. D **22**, 2157 (1980); S.J. Brodsky, SLACPUB- 7604, [arXiv:hep-ph/9708345]; [arXiv:hep-ph/9710288].
- [53] S. J. Brodsky and S. Gardner, SLAC-PUB-14828, 2012.
- [54] J. F. Donoghue and E. Golowich, Phys. Rev. D **15**, 3421 (1977).
- [55] W. C. Chang and J. C. Peng, Phys. Lett. B **704**, 197 (2011) [arXiv:1105.2381 [hep-ph]].
- [56] D. Bourilkov, R. C. Group and M. R. Whalley, hep-ph/0605240.
- [57] M. Botje, Comput. Phys. Commun. **182**, 490 (2011) [arXiv:1005.1481 [hep-ph]].
- [58] Program summary: <http://particles.ipm.ir/links/QCD.htm>.
- [59] T. P. Stavreva and J. F. Owens, Phys. Rev. D **79**, 054017 (2009) [arXiv:0901.3791 [hep-ph]].
- [60] T. Stavreva, I. Schienbein, F. Arleo, K. Kovarik, F. Olness, J. Y. Yu and J. F. Owens, JHEP **1101**, 152 (2011) [arXiv:1012.1178 [hep-ph]].
- [61] V. M. Abazov *et al.* [D0 Collaboration], Phys. Rev. Lett. **102**, 192002 (2009) [arXiv:0901.0739 [hep-ex]].
- [62] T. Aaltonen *et al.* [CDF Collaboration], Phys. Rev. D **81**, 052006 (2010) [arXiv:0912.3453 [hep-ex]].
- [63] J. Alwall, M. Herquet, F. Maltoni, O. Mattelaer and T. Stelzer, JHEP **1106**, 128 (2011) [arXiv:1106.0522 [hep-ph]].